

1995100160
352802

8P N95-14574

MEASUREMENT OF RESISTANCE TO SOLUTE TRANSPORT ACROSS SURFACTANT-LADEN INTERFACES USING A FLUORESCENCE RECOVERY AFTER PHOTBLEACHING (FRAP) TECHNIQUE

Edward P. Browne, Thierry Nivaggioli and T. Alan Hatton
Department of Chemical Engineering
Massachusetts Institute of Technology
Cambridge, MA 02139

ABSTRACT

A non-invasive Fluorescence Recovery After Photobleaching (FRAP) technique is under development to measure interfacial transport in two phase systems without disturbing the interface. The concentration profiles of a probe solute are measured in both phases as a function of time as the system recovers from a perturbation. The perturbation is caused by the irreversible bleaching of a predetermined region on both sides of the interface by an argon-ion laser, and the system relaxation is then monitored by a microscope-mounted CCD camera.

INTRODUCTION

Interfacial transport processes are important in areas as diverse as industrial and analytical separations, tertiary oil recovery, controlled and targeted release drug delivery, and cell membrane transport. However, the mechanism by which these processes takes place is still poorly understood. Solute transport across an interface is influenced by many forces, among them electrostatic, hydrophobic, fluid dynamic and steric interactions. To determine unambiguously the role played by each of these effects requires a reliable technique for the measurement of solute transport resistance under a variety of solution conditions. Unfortunately, to date, no method exists which is both reliable and unambiguous. Techniques which rely on fluid convection, such as the stirred cell [1-4] or the rotating diffusion cell [5], depend on detailed knowledge of the hydrodynamic conditions near the interface. However, such detailed knowledge is rarely available, particularly in surfactant-containing systems. Attempts have been made to eliminate this ambiguity through the use of purely diffusive systems [6, 7], in which transport resistance is measured by monitoring solute concentration profiles as they develop near an interface as a function of time. Most of these techniques suffer from the presence of a blind zone near the interface caused by the meniscus. This blind zone could not be reduced below 200 μm until the work of Aunins [8], in which a photolithography technique was used to produce a blind zone that was only 40 μm thick. An interferometric detection system was used to establish the concentration profiles. Unfortunately, this technique was not very robust, and its scope of applicability was somewhat limited owing to the high solute concentration required. The goal of the present work is to use the photolithography technique of Aunins in conjunction with a perturbation/detection system based on a Fluorescence Recovery After Photobleaching (FRAP) technique [9, 10] to measure resistances to solute interfacial transport unambiguously. FRAP exploits the loss of fluorescence exhibited by certain fluorophores when over-stimulated (photobleaching), so that a system, originally at equilibrium, can be perturbed by strong light and its recovery monitored as it relaxes to a new equilibrium, yielding information about the transport characteristics of the system.

C-5.

2

EXPERIMENTAL

FRAP System

The Fluorescence Recovery After Photobleaching (FRAP) apparatus is shown in Figure 1. In a Video-FRAP experiment, an organic phase and a water phase are placed in a glasswalled cell (1). The system contains a fluorescent probe solute which partitions between the two phases. The cell is allowed to come to equilibrium. The cell is located at the object plane of an epi-illuminated microscope, and the dye molecules are excited by light at 488 nm from a 5W argon-ion laser. The beam splitter / attenuator (2) reduces the power of the laser beam by a factor of 10,000 through multiple partial reflections from four optical flats (3) when its internal shutter (4) is closed. A dichroic mirror (5) reflects the 488 nm-wavelength light onto the cell. The resulting fluorescence emission, being at a longer wavelength, passes through the dichroic mirror and is detected by a CCD camera (6) mounted on the microscope (7 and 8). The effectiveness of the dichroic mirror in differentiating between the excitation and emission wavelengths is enhanced by filters (9 and 10).

Before an experiment begins, the contents of the cell are at equilibrium. To start an experiment, the shutter (4) in the beamsplitter / attenuator opens for approximately 100 ms, exposing the contents of the cell to the laser beam at full power. This results in irreversible photobleaching of some of the fluorophore molecules i.e. the fluorophore no longer fluoresces. A mask (11) is used to define the region of the cell onto which the beam impinges. During photobleaching, the camera is protected by the microscope shutter (12). The recovery of fluorescence in the photobleached region is monitored as a function of time using a Data Translation Frame Grabber, revealing information about the mobility of the fluorescent molecules in each phase and, if the mask is designed to expose a much greater area of one phase than the other during photobleaching, the resistance to interphase transport. The operation of the Video-FRAP system is controlled through a National Instruments PC-based software package (Labview) and data acquisition board.

To obtain sensitive measurements of interfacial resistance, it is necessary to measure solute concentrations as close to the interface as possible. Because the cell walls are made of glass, which is hydrophilic, there would ordinarily be a meniscus between the aqueous and reversed micellar phases, which would distort the fluorescence emission image near the interface. To minimize the size of the meniscus, the surface of the glass cell wall is treated by a photolithography technique so that the lower part of the wall (corresponding to the water phase) is hydrophilic, and the upper part of the wall is hydrophobic. As a result, when the cell is filled appropriately, a 90° contact angle is obtained. Menisci as shallow as 25 μm have been obtained with this method.

DATA ANALYSIS

To obtain concentration profiles from the two-dimensional images of the fluorescence recovery that are stored in the frame grabber, the images are calibrated with an image taken before photobleaching, when all concentrations were known.

The two-dimensional unsteady state diffusion equation is solved using a Crank-Nicholson alternating-direction implicit finite difference scheme [11, 12], with the interfacial resistance, R , as a variable parameter which is introduced in the boundary conditions. The experimental interfacial resistance is obtained by finding the R value which results in the best fit of the diffusion equation to the experimental concentration profiles via a Newton-Raphson iteration scheme.

The diffusion coefficients of fluorophore in both the aqueous phase and the organic phase are measured directly in the diffusion cell.

PRELIMINARY RESULTS

Preliminary experiments were carried out with an aqueous phase consisting of 10 μM fluorescein (the probe solute) and 200 mM sodium chloride, and a reversed-micellar organic phase consisting of heptane with 200 mM AOT surfactant. The system was allowed to come to equilibrium, with the fluorescein distributing between the two phases. Photobleaching took place for 300 ms, and although the bleaching beam was somewhat ill-defined in these preliminary experiments, most of the photobleaching occurred in the aqueous phase.

Figure 2(a) shows the initial, post-bleach, two-dimensional concentration profile in false color. The concentrations have been normalized, so that a value of 1.0 (dark blue in figure 2(a)) represents no change in probe solute fluorescence between the pre-bleach image and the post-bleach image. The maximum photobleaching that occurred was 10%, represented by a normalized concentration of 0.9 (red in figure 2(a)).

The situation one minute after bleaching is shown in Figure 2(b). The system has started to relax from its immediate, post-bleach state, as seen by the false color image becoming less 'red'. At longer times, the image will eventually become blue, as the fluorescence intensity returns to its pre-bleach value.

Figure 3 shows the one-dimensional concentration profiles normal to the interface obtained by averaging the two-dimensional concentration fields. The data contain a large amount of noise, so it was not possible to obtain an interfacial resistance value for this preliminary experiment. However, the process of relaxation can clearly be seen in the aqueous phase, as the system returns to equilibrium.

FUTURE WORK

The system is currently being optimized to reduce noise in the fluorescence images. The first complete set of experiments will measure the rates of extraction and reextraction of fluorescein into and out of an AOT reversed-micellar phase in contact with an aqueous phase as a function of the aqueous ionic strength. This will illustrate the role charge interactions play in reversed micellar solubilization [2].

The sensitivity of the technique could be much improved by an increase in the amount of photobleaching. Unfortunately, buoyancy driven convection occurs at higher levels of photobleaching, which tends to mask the purely diffusive process. This restriction can, however, be removed by operating in a microgravity environment.

CONCLUSIONS

The apparatus is in the final stages of construction, and is currently being tested and its operational parameters optimized. Preliminary experiments indicate that this approach will provide a reliable technique for investigating solute transport in surfactant-containing systems free of the ambiguity that is inherent in convective systems, and that the performance of the system can be much enhanced by operation in a microgravity environment.

ACKNOWLEDGEMENTS

The authors would like to thank the staff of the Microelectronics Laboratory at the Center for Materials Science and Engineering (CMSE) at MIT for their help with the photolithography procedure.

REFERENCES

1. Lewis, J.B., "The Mechanism of Solute Transport across Liquid-Liquid Interfaces . I. The Determination of Individual Mass Transfer Coefficients of Binary Systems." *Chemical Engineering Science*, **3** (1954), pp. 218-259.
2. Nitsch, W. and Plucinski, P., "Two-Phase Kinetics of Solubilization in Reversed Micelles" *Journal of Colloid and Interface Science*, **136** (1990), pp. 338-351.
3. Dungan, S.R., Bausch, T., Hatton, T.A., Plucinski, P., and Nitsch, W., "Interfacial Transport Processes in the Reversed Micellar Extraction of Proteins" *Journal of Colloid and Interface Science*, **145** (1991), pp. 33-49.
4. Plucinski, P. and Nitsch, W., "Mechanism of Mass Transfer between Aqueous Phase and Water-in-Oil Microemulsion" *Langmuir*, **10** (1994), pp. 371-376.
5. Albery, W.J., Choudhery, R.A., Atay, N.Z., and Robinson, B.H., "Rotating Diffusion Cell Studies of Microemulsion Kinetics" *Journal of the Chemical Society, Faraday Transactions I*, **83** (1987), pp. 2407-2419.
6. Ward, A.F.H. and Brooks, L.H., "Diffusion Across Interfaces" *Transactions of the Faraday Society*, **48** (1952), pp. 1124.
7. Chandrasekhar, S. and Hoelscher, H.E., "Mass Transfer Studies Across Liquid/Liquid Interfaces" *AIChE Journal*, **21** (1975), pp. 103.
8. Aunins, A.H., *Solute Transport Across Surfactant Laden Interfaces: Developement of a Novel Interferometric Technique for Measuring Interfacial Resistance*, Ph.D. Thesis, Massachusetts Institute of Technology, Cambridge MA, 1991.
9. Koppel, D.E., Axelrod, D., Schlessinger, J., Elson, E.L., and Webb, W.W., "Dynamics of Fluorescence Marker Concentration as a Probe of Mobility" *Biophysical Journal*, **16** (1976), pp. 1315-1329.
10. Wolf, D.E., *Designing, Building, and Using a Fluorescence Recovery after Photobleaching Instrument*, in *Methods in Cell Biology*, Academic Press: 1989, pp. 271-306.
11. Crank, J., *The Mathematics of Diffusion*, 2nd ed., London: Oxford University Press, 1975.
12. Gerald, C.F. and Wheatley, P.O., *Applied Numerical Analysis*, 3rd ed., Addison-Wesley, 1984.

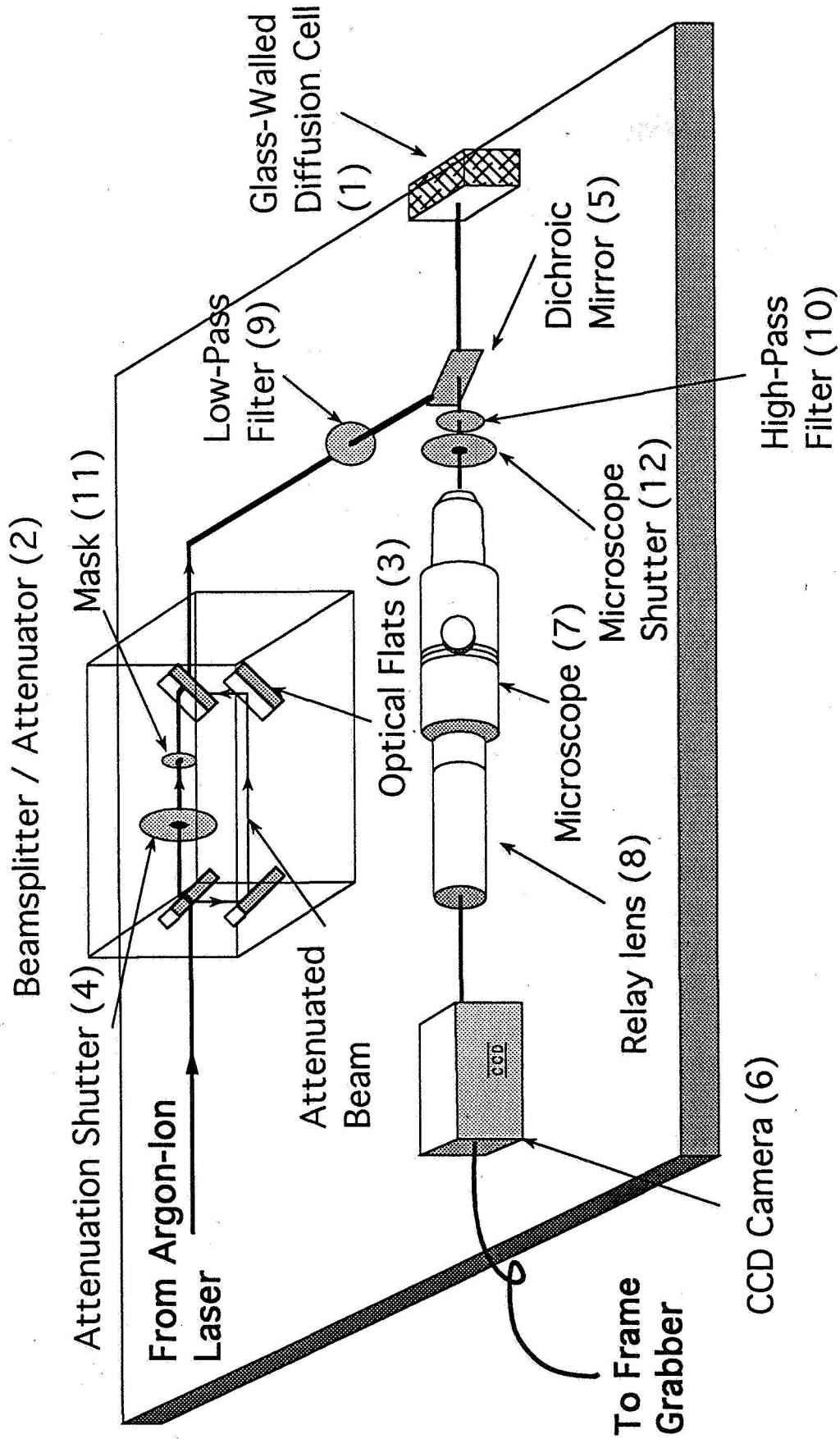


Figure 1. Video-FRAP System

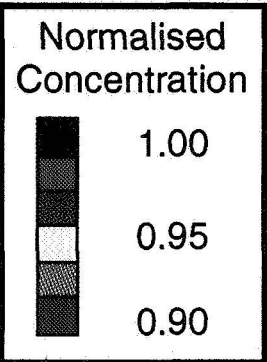
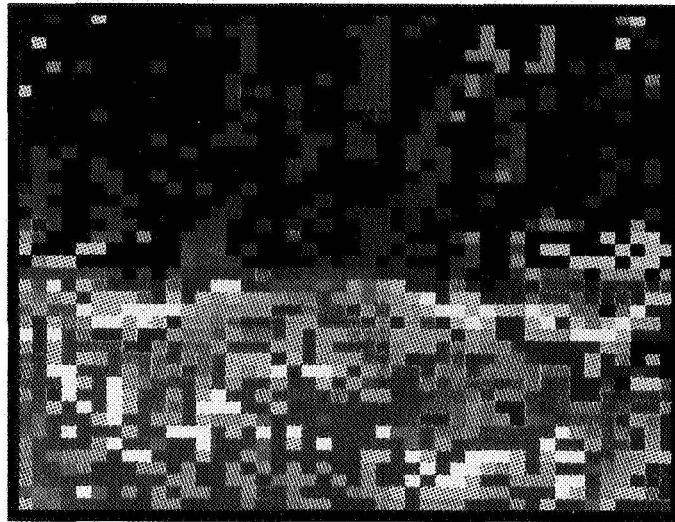
Figure 2(a)

t = 0 sec

Water Phase

Interface

Oil Phase



Field of View:
1mm x 1mm

Figure 2(b)

t = 60 sec

Water Phase

Interface

Oil Phase

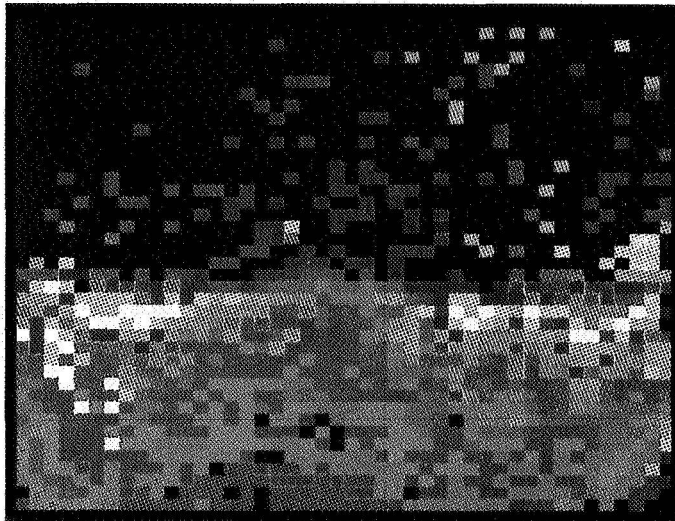


Figure 3

